

In vitro mapping of ^1H ultrashort T_2 and T_2^* of porcine menisci: analysis of the signal decay reveals collagenous fibril texture

Stefan Kirsch¹, Michael Kreinest², Gregor Reisig², and Lothar R Schad¹

¹Computer Assisted Clinical Medicine, Medical Faculty Mannheim, Heidelberg University, Germany, ²Department for Experimental Orthopaedics and Trauma Surgery, University Medical Centre Mannheim, Heidelberg University, Mannheim, Germany

Introduction

Recently, a method for single-slice mapping of ultrashort T_2 was presented [1]. In this study, the method was used to investigate mapping of ultrashort T_2 of porcine menisci. The T_2 maps were compared to T_2^* maps. Water protons in collagen rich tissue are subject to dipole-dipole coupling, restricted diffusion, multiple compartments and mesoscopic magnetic field inhomogeneities originating from the collagenous fibril texture. Since T_2 and T_2^* relaxation of the magnetization in such an environment can yield non-exponential (Gaussian approximation) signal decays [2-4], we used 3 different analytical functions for the curve fitting procedure: (a) monoexponential decay (ME), (b) biexponential decay (BIE), and (c) a superposition of a Gaussian decay and an exponential decay (GE). The quality of the curve fits was estimated and visualized by calculating the reduced chi-squared (χ^2_{red} , "goodness of fit") for each pixel in the T_2 and T_2^* maps.

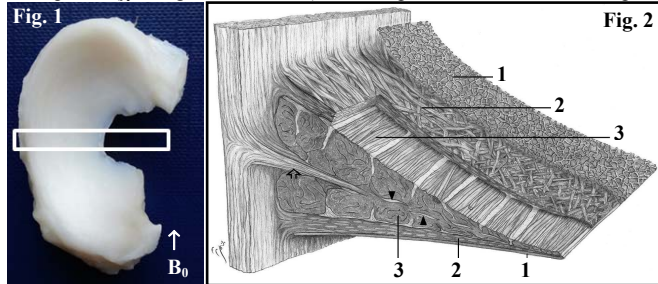
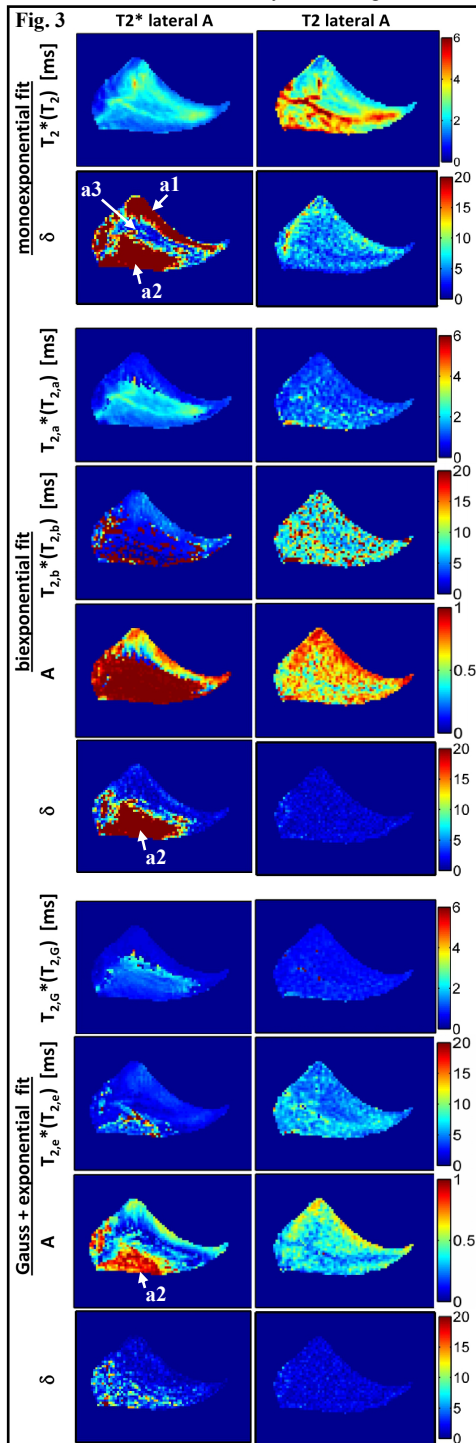


Fig. 2 Cross section of the human meniscus (taken from Ref. [5]). Regions with different collagenous texture are indicated: (1) superficial network with random fibril orientation, (2) lamellar layer with radial fibrils, (3) central main layer where fibrils are oriented in a circular manner.

Material and Methods

T_2 and T_2^* maps were acquired for 8 acutely isolated porcine menisci (4 medial, 4 lateral). T_2 mapping was performed according to Ref. [1]. For each meniscus one central slice was mapped (see Fig. 1 for slice position). Parameters for the T_2 mapping: TR = 140 ms, slice thickness = 2 mm, FOV = (35 × 35) mm², matrix = 128 × 128, BW = 1.2 kHz/pixel, number of projections = 322, TE = (0.45 - 10.45) ms with 35 increments. T_2^* mapping was performed using a 2D-UTE rf pulse sequence with variable acquisition delay t_d . Parameters for the T_2^* mapping were the same as in the T_2 mapping, except for t_d = (0.2 - 10.2) ms with 35 increments. All the experiments were performed on a 9.4 T Bruker Biospec 94/20 USR small animal system. A ^1H quadrature resonator with a diameter of 7.2 cm was used in Tx/Rx mode. The measured signal decay was fitted by

(a) $S(TE) = S_0 \cdot \exp(-TE/T_2^*)$, (b) $S(TE) = S_0[A \cdot \exp(-TE/T_{2,a}^*) + (1-A) \cdot \exp(-TE/T_{2,b}^*)]$,

(c) $S(TE) = S_0[A \cdot \exp(-0.3606 \cdot (TE/T_{2,G}^*)^2) + (1-A) \cdot \exp(-TE/T_{2,e}^*)]$,

where $1/[\pi T_{2,G}^*]$ is the FWHM of the corresponding Gaussian lineshape in the frequency domain. In order to estimate and visualize the quality of the fit, the value $\delta = |1 - \chi^2_{\text{red}}|$ was calculated. It is well known that $\chi^2_{\text{red}} = 1$ indicates that the extent of the match between observations and estimates is in accord with the error variance. For high values of χ^2_{red} the model does not fully capture the data. $\delta \rightarrow 0$ indicates an acceptable match between the measured data and the fit.

Results

Fig. 3 shows the parameter maps for the different fit models on an exemplary chosen lateral porcine meniscus (left column T_2^* , right column T_2). In the T_2^* measurements very high values of δ are observed for the ME and BIE fit in the femoral area (a1) and in the tibial area (a2). However, the T_2^* map of the ME fit also shows low values of δ in the middle area (a3). In this area the signal decay is well described by a ME decay. In contrast to the ME and BIE fit the GE fit shows overall low values of δ . From the fraction map (A values) of the GE fit it can be concluded that in the femoral and tibial area the signal decays exhibit a significant Gaussian component (which was verified by visual inspection of individual pixel-decays). Compared to the T_2^* maps the T_2 maps show low values of δ for all fit functions used. Interestingly, the T_2^* and the T_2 maps show significant differences. This phenomenon is addressed to the different dephasing mechanisms involved in the T_2^* and T_2 signal decay. For all 8 menisci investigated, the GE fit shows best overall match with the measured data in the T_2^* measurements. The BIE and the GE fits show similar good performance in the T_2 measurements.

Discussion & Conclusion

For the interpretation of the parameter maps we assume that porcine and human menisci have comparable composition, because both menisci are subject to similar mechanical forces. Comparison of the fraction map (A values) of the GE fit with the composition of human menisci (Fig. 2) suggests that the areas a1, a2 and a3 (Fig. 3) can be assigned to regions with different collagenous texture: (a1) femoral area → superficial network and lamellar layer, (a2) tibial area → lamellar layer with radial fibrils, (a3) middle area → central area with circular fibrils. This speculation is supported by theory [2-4], since Gaussian-like signal decays are expected in a network of cylinders where the length axes of the cylinders are oriented randomly (superficial fibril network) or perpendicular (tibial area) to the B_0 direction. A ME decay is expected when the cylinders are oriented parallel to B_0 (middle area). The different appearance of the fraction maps (A values) of the T_2^* and T_2 GE fit also support this interpretation, since the spin echo should partially refocus the spin dephasing owing to the collagenous fibril network (→ almost no Gaussian component visible in the tibial area in the fraction map (A values) of the T_2 GE fit). In future, *in-vivo* mapping of ultrashort T_2^*/T_2 may provide a tool for early detection of meniscal tissue degeneration. However, further studies involving histology and localized *in vitro* tissue degeneration models will be necessary to verify the information content of the T_2^*/T_2 maps.

References

- [1] S. Kirsch *et al.* JMR 210 (2011) 133-136; [2] D. A. Yablonskiy *et al.* MRM 32 (1994) 749-763
- [3] A. L. Sukstanskii *et al.*, JMR 163 (2003) 236-247; [4] A. L. Sukstanskii *et al.*, JMR 157(1) (2002) 92-105
- [5] W. Petersen *et al.*, Anat Embryol 197 (1998) 317-324.